Biuletyn WAT
Vol. LXVII, Nr 4, 2018

Stress wave method in dynamic resistance analysis of an explosion-proof valve

BARTŁOMIEJ PIEŃKO, ZBIGNIEW SZCZEŚNIAK

Military University of Technology, Faculty of Civil Engineering and Geodesy,
2 Gen. W. Urbanowicza Str., 00-908 Warsaw, Poland,
bartlomiej.pienko@wat.edu.pl, zbigniew.szczesniak@wat.edu.pl

Abstract. The paper presents the concept of a novel stress wave method (SWM) for determining the dynamic reaction of structural elements of an explosion-proof valve. The stress wave method is an original solution to the issue of the dynamic reaction of structural elements and systems. It is particularly recommended in the case of intensive percussive or explosive impacts. The method was developed by the author of works [14, 15]. It reflects the wave nature of stress development. The paper presents the origin, assumptions and the basic dependencies of the method. The characteristics of the method are illustrated by means of solutions to issues closely related to the requirements for testing the resistance of shelter explosion-proof valves. The description also includes a comparison of the calculation results with the results obtained by the finite element method (FEM) and the results of experimental tests. The possibility of significant differences between the compared solutions has been shown. It should be noted that geometric attenuation, reflections and interference of waves are natural for the dynamic reaction of an element and therefore for wave processes. These phenomena can significantly affect the distribution of the parameters of the sought dynamic reaction in space and time. The proposed method of analysis is distinguished by high accuracy of calculations.
Keywords: stress waves, structural element vibrations, discrete models, differential solution, explosion-proof valve
DOI: 10.5604/01.3001.0012.8497

1. Introduction

The explosion-proof valves considered in the paper are used in shelter installations and belong to the basic protective elements of a given facility. They are used mainly to protect ventilation ducts from an air shock wave.

The general principle of the explosion-proof valve operation is closing the working cross-section at the moment of a sudden increase in air overpressure (Fig. 1.1).

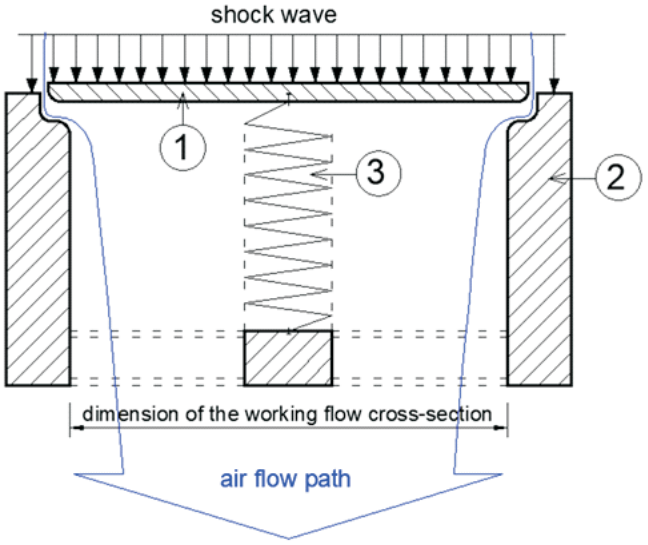

Fig. 1.1. Principle of operation of the explosion-proof valve: 1 — moving closing element, 2 — fixed stopper element, 3 — spring

Fig. 1.2. Main components of a explosion-proof valve:
1 — stopper grate, 2 — moving grate, 3 – body

A new generation automatic explosion-proof valve design was developed at the Faculty of Civil Engineering and Geodesy of the Military University of Technology as part of research and development work. The basic valve assemblies include a stopper grate, a moving grate, the body and an electronic control system (Fig. 1.2).

The valve's actuation system, consisting of structural elements and mechanisms, must have mechanical resistance adequate for the conditions induced by the shock wave generated by a given explosion. Various commercial numerical programs developed for structural mechanics may be used to design explosion-proof valve elements. We propose a new non-commercial stress wave method (SWM) for the analysis of dynamic reaction of structural elements and systems which has high accuracy of calculations. In one-dimensional terms, simulations have zero-method error.

A description of the method and its features will be presented below. We will illustrate the essence and significance of the wave process in the material field of a given structure. We will present selected elements of the analysis of dynamic resistance of a valve stopper rib induced by an air shock wave and in the conditions of a collision of the basic valve ribs.

2. Valve dynamic resistance analysis method

Modern structure mechanics uses a number of calculation methods, most notably the FEM and the finite difference method (FDM). In [16], it was shown that FEM cannot be used to fully reflect the wave nature of stress development. Therefore, we will propose a method of analysis, the basic component of which is an original numerical model to simulate the propagation of stress waves, with a spatial dimension selected according to the conditions of a given task. The mapping of the wave nature of stress development is particularly recommended for cases related to impact-type actions.

The considered structural elements of the valve are subjected to such impacts as shock wave, collision of components and special kinematic actions. The abovementioned actions generate distortions in the structural material that propagate in the form of stress waves and strains. We seek parameters of the wave process, assuming the continuity of the medium constituting the structural material. The equations for the ponderable motion of an infinitesimal rectangular element are as follows:

$$\frac{\partial \sigma_{xx}}{\partial x} + \frac{\partial \tau_{xy}}{\partial y} + \frac{\partial \tau_{xz}}{\partial z} - \rho \frac{\partial^2 u_x}{\partial t^2} = 0 \tag{2.1}$$

$$\frac{\partial \tau_{xy}}{\partial x} + \frac{\partial \sigma_{yy}}{\partial y} + \frac{\partial \tau_{yz}}{\partial z} - \rho \frac{\partial^2 v_y}{\partial t^2} = 0 \tag{2.2}$$

$$\frac{\partial \tau_{zx}}{\partial x} + \frac{\partial \tau_{zy}}{\partial y} + \frac{\partial \sigma_{zz}}{\partial z} - \rho \frac{\partial^2 w_z}{\partial t^2} = 0 \tag{2.3}$$

where: ρ is the medium density,
u, v, w — displacements in the x, y, z direction, respectively,
σ_{xx}, σ_{yy}, σ_{zz} — normal stress in the x, y, z direction, respectively,
τ_{xy}, τ_{xz}, τ_{zy} — tangential stress in the xy, xz, yz plane, respectively.

The equations above can be transformed into wave equations of dilatation θ and rotation $\vec{\omega}$ for a homogeneous and isotropic medium reacting in accordance with linear strain-displacement relations with respect to linear elasticity. These equations are as follows:

$$\nabla^2 \theta = \frac{1}{a_1^2} \frac{\partial^2 \theta}{\partial t^2} \tag{2.4}$$

$$\nabla^2 \vec{\omega} = \frac{1}{a_2^2} \frac{\partial^2 \vec{\omega}}{\partial t^2} \tag{2.5}$$

where: $a_1 = \sqrt{\dfrac{\lambda + 2\mu}{\rho}}$ is dilatational wave speed,

$a_2 = \sqrt{\dfrac{\mu}{\rho}}$ — rotational wave speed,

λ, μ are Lamé's constants.

The above equations (2.4 i 2.5), which have the same structures, differ in wave speed, with $a_1 > a_2$.

In the formulation of a given problem, these equations should be supplemented with boundary, initial and compliance conditions.

The nature of the material waves considered here, which are defined by equations (2.4) and (2.5), can be depicted within a differential grid where every element has the dimensions $\Delta x = \Delta y = \Delta z = h$. Hence, the element mass will be $\Delta m = \rho h^3$. We will place the calculated mass as aggregated in the centre of each elemental plane abcd as in the spatial sketch of the discussed grid presented in Fig. 2.1. A sketch of the mass distribution for the two-dimensional case is given in Fig. 2.2.

Mass distribution within each basic element, presented in two dimensions in Fig. 2.3., is of particular significance in the proposed method. This distribution is distinguished by the division of the whole mass into two halves in each direction.

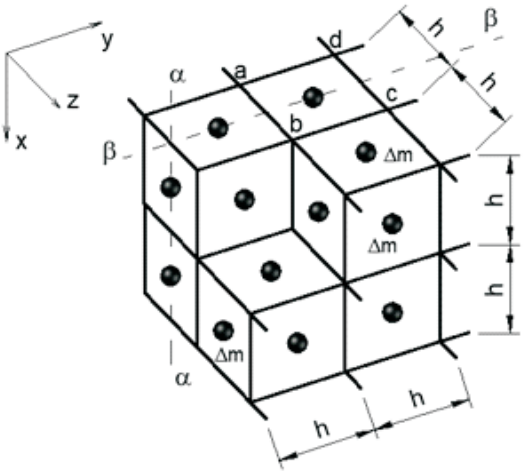

Fig. 2.1. Sketch of the spatial distribution of aggregate masses

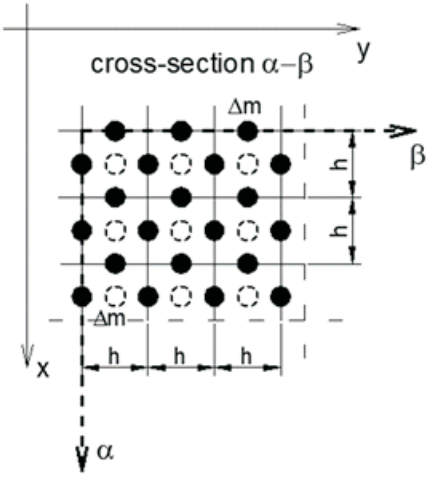

Fig. 2.2. Sketch of the distribution of aggregate masses at a cross-section with the α-β plane

The need for such a division was demonstrated in [1], which was concerned with a one-dimensional model.

The proposed approach is a result of an analysis of the conditions of error-free differential approximation of the wave problem. The framework of a two-dimensional model is determined by a square grid with the mesh size $h \times h$ covering a given wave field. The rules for numbering grid lines and individual fields are shown in Fig. 2.4.

Note also that the structure of the basic element of the model with the dimensions $h \times h$ is obtained as a result of a mental intersection of two one-dimensional wave bands in the field of a given element (see Fig. 2.3). We have taken into account the natural possibility of simultaneous displacement of the mass of the medium Δm contained in the elementary $h \times h$ field in both the x and y direction. In the case of the two-dimensional model, the distinctive mass is:

$$\Delta m = b\, h^2\, \rho \tag{2.6}$$

where b is the dimension of the model in the z direction.

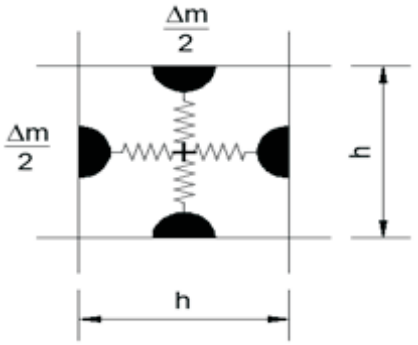

Fig. 2.3. Mass distribution in a field of the basic two-dimensional element

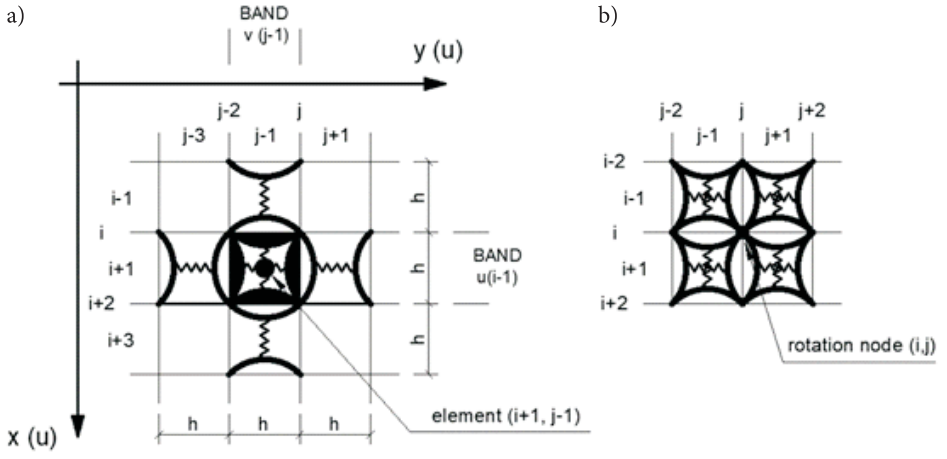

Fig. 2.4. Basic components of the two-dimensional model:
a) — structure of the elementary field $h \times h$, b) — rotational node

Apart from the dilatational movement, the two-dimensional model also reflects the motion resulting in rotational strain. The local axis of rotational motion passes through the point where four elementary fields meet, referred to as the node, in relation to which four masses of the model rotate (see Fig. 2.4b).

The half-masses were connected by flexible elements – "springs" – which schematically reflect the strain possibilities of a given medium. The intersection of springs symbolizes the strain interdependence of directions, which in the case of a homogeneous and isotropic elastic body is expressed by generalized Hooke's law.

In the discussed two-dimensional situation, this law can be captured as follows:

$$\sigma_{\alpha\beta}^{n} = 2\mu\varepsilon_{\alpha\beta}^{n} + \lambda\theta_{\alpha\beta}^{n}, \tag{2.7}$$

$$\tau_{\alpha\beta}^{n} = \mu\gamma_{\alpha\beta}^{n} \tag{2.8}$$

where: $\varepsilon_{\alpha\beta}^{n}, \theta_{\alpha\beta}^{n}, \gamma_{\alpha\beta}^{n}$ — symbolize longitudinal, dilatational and rotational strains, respectively,
$\sigma_{\alpha\beta}^{n}$, $\tau_{\alpha\beta}^{n}$ — normal, shear stresses.

In the analysis of the reaction of structural elements subjected to intensive dynamic impact or blast loads, the elastic reaction phase of the material may be prolonged compared to the static reaction. The result is a delay in the occurrence of inelastic reaction and, at the same time, an increase in the dynamic level of the elastic limit. This limit is also called the upper yield limit. The effect in question is called plastic delay and its existence limits the time of the delay t_d, which depends on the existence of a change in the strain rate and the location of a specific material point within a given element. If the time of reaching the maximum elastic strain t_m will be less than the plastic delay time t_d, then the reaction of the material can be described only by means of the dependence (2.7). The ability to meet this condition, that is $t_m \leq t_d$, is verified using Campbell's dynamic plasticity criterion:

$$\int_0^{t_d} \left\{ \frac{\sqrt{J_2\left[\sigma_{ij}(t)\right]}}{K_0} \right\}^{\alpha} dt = t_0, \tag{2.9}$$

where: K_0, α, t_0 — are material constants,
$J_2 = \frac{1}{2} S_{ij} S_{ij}$ — the second invariant of the stress deviator.

When the dynamic plasticity criterion is met, the plastic delay time and the dynamic plasticity area are determined:

$$\sqrt{J_{2d}} = \sqrt{J_2\left[\sigma_{ij}(t_d)\right]} \geq K_0 \tag{2.10}$$

However, if the condition $t_m \geq t_d$ is met, the material reaction will take place in the viscoplastic flow phase. This phase is characterized by the existence of the lower yield point. The discussed effects can be illustrated using the results of experimental tests of mild steel in the form of $\sigma - \varepsilon$ relationship for various strain rates (see Fig. 2.5). The test results were taken from the website [18]. The steel showed a pronounced upper and lower yield point effect. It did not exhibit strain reinforcement after plasticization to any significant extent. The ideal viscoplastic flow involved the strain range of up to about 8%.

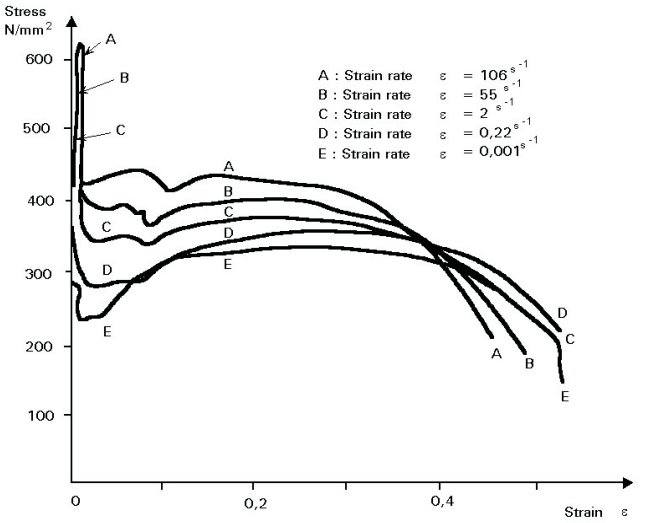

Fig. 2.5. Influence of strain rate on the mechanical properties of mild steel [18]

In this paper, we will not consider the reaction of the valve element in the inelastic phase due to the functional conditions of the whole device. Therefore, we adopt Campbell's criterion as the basis for the evaluation of the valve resistance.

The elementary internal longitudinal forces of the model occur in springs and we mark them as S_u^n and S_v^n according to their directions. Index n means isolated time t^n with time steps Δt, because $t^n = n\,\Delta t$.

Elementary tangential forces are distributed along the grid lines, which are the trace of the central planes of the model's masses. According to the direction, we will mark them with symbols T_u^n and T_v^n.

The (i, j-1) mass motion equation in the direction of the x axis is as follows:

$$\Delta m \ddot{u}_{i,j-1}^{n,n+1} = S_{U(i+1,j-1)}^n - S_{U(i-1,j-1)}^n + T_{UD(i-1,j)}^n + T_{UG(i+1,j)}^n - T_{UD(i-1,j-2)}^n - T_{UG(i+1,j-2)}^n \quad (2.11)$$

The (*i*-1,*j*) mass motion equation in the direction of the *y* axis:

$$\Delta m\ddot{v}_{i-1,j}^{n,n+1} = S_{V(i-1,j+1)}^{n} - S_{V(i-1,j-1)}^{n} + T_{VP(i,j-1)}^{n} + T_{VL(i,j+1)}^{n} - T_{VP(i-2,j-1)}^{n} - T_{VL(i-2,j+1)}^{n} \tag{2.12}$$

Longitudinal strain in "springs" within area (*i*-1, *j*-1):

$$\varepsilon_{U(i-1,j-1)}^{n} = \frac{u_{(i,j-1)}^{n} - u_{(i-2,j-1)}^{n}}{h} \tag{2.13}$$

$$\varepsilon_{V(i-1,j-1)}^{n} = \frac{v_{(i-1,j)}^{n} - v_{(i-1,j-2)}^{n}}{h} \tag{2.14}$$

Rotational strain $\gamma_{(i,j)}^{n}$ in node (i, j) caused by rotary motion may be expressed as follows:

$$\gamma_{(i,j)}^{n} = \frac{u_{(i,j+1)}^{n} - u_{(i,j-1)}^{n} + v_{(i+1,j)}^{n} - v_{(i-1,j)}^{n}}{h} \tag{2.15}$$

The forces in "springs" within area (*i*-1, *j*-1) are:

$$S_{U(i-1,j-1)}^{n} = \sigma_{U(i-1,j-1)}^{n} bh \tag{2.16}$$

$$S_{V(i-1,j-1)}^{n} = \sigma_{V(i-1,j-1)}^{n} bh \tag{2.17}$$

Where normal stresses are:

$$\sigma_{U(i-1,j-1)}^{n} = 2\mu\varepsilon_{U(i-1,j-1)}^{n} + \lambda\theta_{(i-1,j-1)}^{n} \tag{2.18}$$

$$\sigma_{V(i-1,j-1)}^{n} = 2\mu\varepsilon_{V(i-1,j-1)}^{n} + \lambda\theta_{(i-1,j-1)}^{n} \tag{2.19}$$

$$\theta_{(i-1,j-1)}^{n} = \varepsilon_{U(i-1,j-1)}^{n} + \varepsilon_{V(i-1,j-1)}^{n} \tag{2.20}$$

Tangential stress $\tau_{(i,j)}^{n}$ in node (i, j) will be obtained from the relationship:

$$\tau_{(i,j)}^{n} = \mu\gamma_{(i,j)}^{n}. \tag{2.21}$$

Along the vertical plane, there are forces $T_{UG(i-1,j)}^{n}$ and $T_{UD(i-1,j)}^{n}$ acting between nodes (*i*-2, *j*) and (i, j), whose values are:

$$T_{UG(i-1,j)}^{n} = \frac{\left(3\tau_{(i-2,j)}^{n} + \tau_{(i,j)}^{n}\right)bh}{8} \tag{2.22}$$

$$T_{UD(i-1,j)}^{n} = \frac{\left(3\tau_{(i,j)}^{n} + \tau_{(i-2,j)}^{n}\right)bh}{8} \tag{2.23}$$

Along the horizontal plane, there are forces $T^n_{VL(i,j-1)}$ and $T^n_{VP(i,j-1)}$ acting between nodes (*i*,*j*-2) and (*i*,*j*), whose values are:

$$T^n_{VL(i,j-1)} = \frac{\left(3\tau^n_{(i,j-2)} + \tau^n_{(i,j)}\right)bh}{8} \tag{2.24}$$

$$T^n_{VP(i,j-1)} = \frac{\left(3\tau^n_{(i,j)} + \tau^n_{(i,j-2)}\right)bh}{8} \tag{2.25}$$

To integrate the equations of motion at time, we will use the explicit finite difference scheme while respecting the Courant–Friedrichs–Lewy stability condition (see [17]):

$$\Delta t \leq \frac{1}{\sqrt{N}} \frac{h}{a_{max}},$$

where N is the dimension of the considered wave-vector space.

3. Characteristics of selected properties of the stress wave method

3.1. Wave effects induced in a structural element

In order to illustrate the possibilities of the SWM method in respect of the simulation of the process of stress wave propagation in structures, numerical calculations of the effort of a shield element with a length of 200 cm and a height of 50 cm were carried out (Fig. 3.1a). The shield, treated as supported with bilateral joints, was impact-loaded with a 50 MPa overpressure for 100 μs (Fig. 3.1b). The discretization of the element's volume was carried out using a two-dimensional grid with a mesh size of h = 1 cm. Young's modulus of 210 GPa, 0.3 Poisson's ratio and the material density of 7860 kg/m^3 were adopted for the calculations. The time step adopted for the numerical calculations was Δt = 0.589 μs.

Figures 3.2 and 3.3 present maps of the distribution of normal stress acting in the direction of the external load $p(t)$. Normal stress maps were made at 29.45 μs (Fig. 3.2) and 117.80 μs (Fig. 3.3), counting from the beginning of the loading process. They show the process of stress wave propagation. A characteristic feature of the method is the possibility to take into account interference of stress waves, for example as a result of reflection from a free edge (Fig. 3.3).

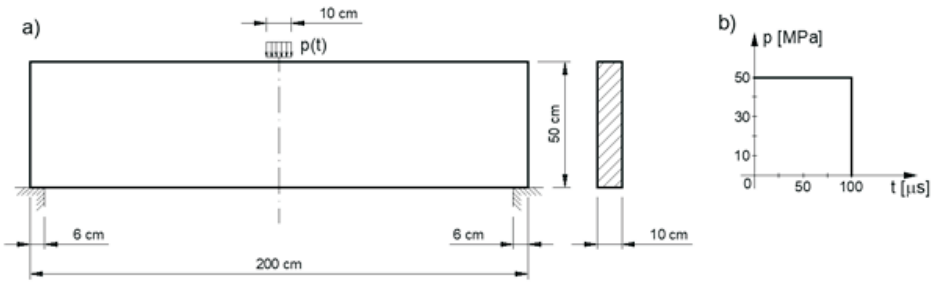

Fig. 3.1. Shield element: a) — geometric characteristics and boundary conditions, b) — characteristics of load change over time

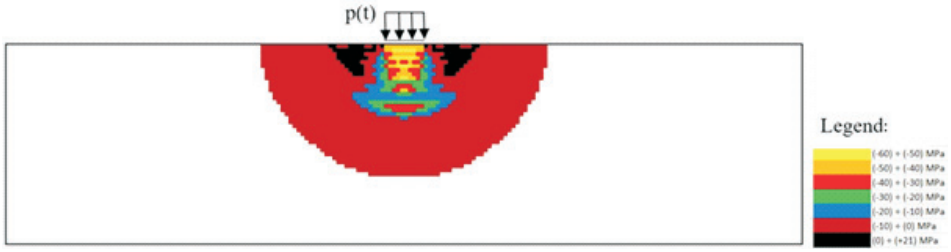

Fig. 3.2. Distribution of normal stresses acting in the direction of the load $p(t)$ in the analysed disc at 29.45 μs

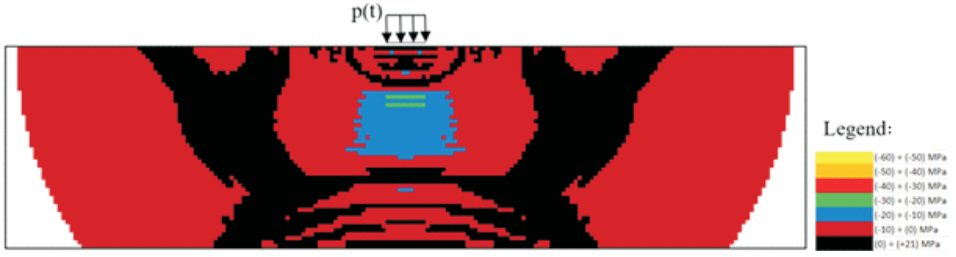

Fig. 3.3. Distribution of normal stresses acting in the direction of the load $p(t)$ in the analysed shield at 117.80 μs

3.2. Stopper rib reaction to the impact of an air shock wave

We will present an analysis of the dynamic reaction of a valve stopper rib using the stress wave method. The stopper rib has the form of a shield with inside span l = 656 mm, height h = 310 mm and thickness b = 34 mm. The spacing of ribs is a = 30 mm. The conditions of the structural connection of the rib to the massive valve body can be identified as rigid attachment along the entire height of the rib. The analysis takes into account the case of fixed full contact of the moving rib to the

stopper rib, which is ensured by the valve mechanisms during the closing phase. The stopper ribs were made of low carbon steel with a characteristic tensile strength of 550 MPa. Young's modulus of 210 Gpa, 0.3 Poisson's ratio and the material density of 7810 kg/m^3 were adopted for the calculations. It was assumed that the maximum overpressure on the front of the air shock wave is 6.7 MPa, which after reflection from the surface of the closed valve gives an overpressure of 50 MPa. Overpressure was assumed to be fixed all the time.

The disc model of the rib was used for the calculations. The calculations were made assuming spatial and temporal discretization with the parameters $h = 4$ mm, $\Delta t = 0.4$ μs. The numbering of the elements of the adopted grid in the wave field of the main rib is illustrated in Fig. 3.4.

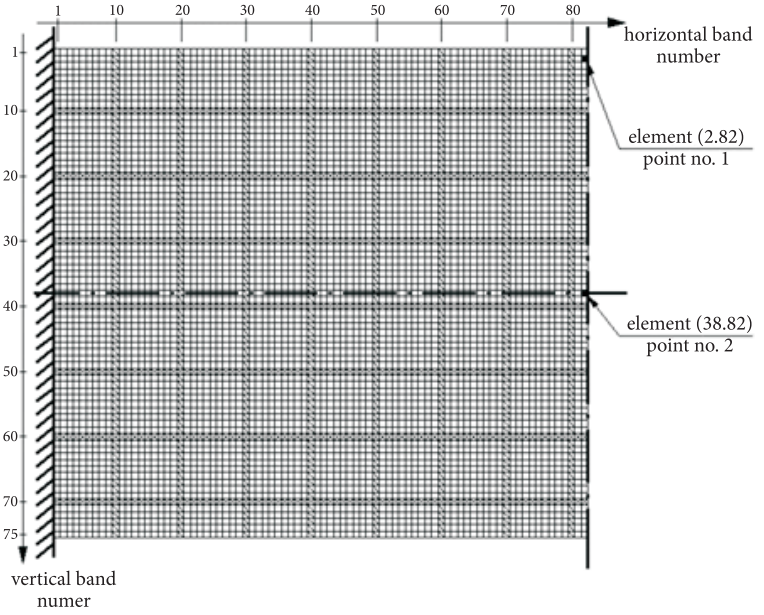

Fig. 3.4. Numbering of the grid elements in the main rib's wave field

The state of the rib material effort was evaluated on the basis of reduced stresses determined according to the Huber–Mises strength hypothesis. We will present values of the discussed stresses for points 1 and 2 (see Fig. 3.4).

As a result of the calculations using the SWM method, the greatest effort was found at point 1 of the support cross-section. The maximum reduced stresses reached the value of $\sigma_{r1} = 638.59$ MPa, which is illustrated in Figure 3.5. In this cross-section, no plastic strains were found despite exceeding the static yield point. This is an obvious consequence of the included plastic delay effect. In the central

cross-section, the greatest effort was obtained at point 2 of the loaded edge. The maximum reduced stresses reached the value σ_{r2} = 188.6 MPa, which is illustrated in Figure 3.6.

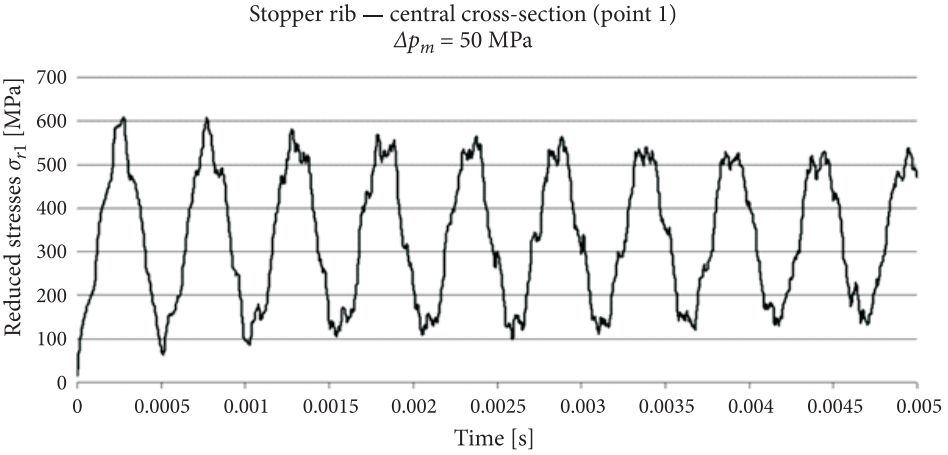

Fig. 3.5. Change in reduced stress σ_{r1} over time

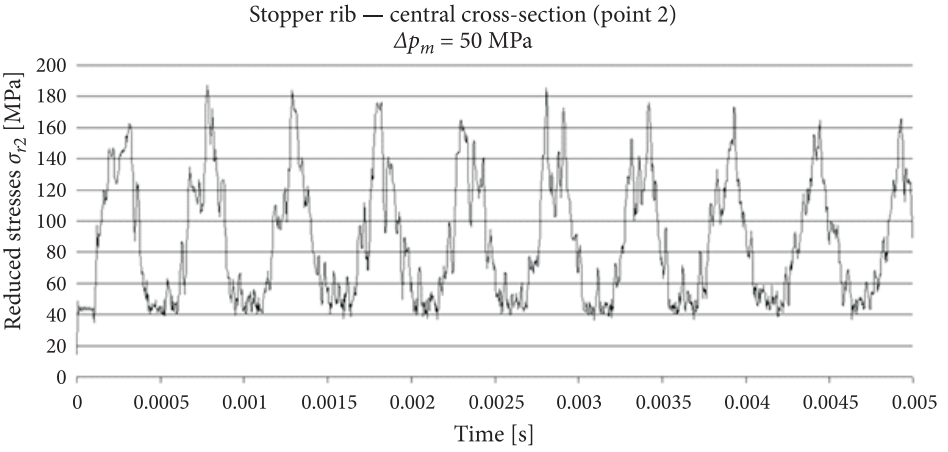

Fig. 3.6. Change in reduced stress σ_{r2} over time

For the purposes of comparison, an analysis of the dynamic reaction of the rib was performed using the FEM. The geometry of the valve body with ribs was described by means of a grid with 130,000 three-dimensional, 10-node finite elements of the "tetrahedron" type and five integration points. The elastic-perfectly plastic model was used to describe the strain properties of the structural material. Based on the results obtained in the analysis by the SWM, an increase in the yield

point to 630 MPa was assumed. The level of material effort is represented by means of reduced stresses calculated according to the Huber–Mises hypothesis. The results are shown in Figure 3.7. It was found that inelastic changes in the material reaction are negligible. However, it can be noticed that the state of material effort, determined taking into account the wave nature of stress development, is significantly different in comparison to the FEM calculations in the central part of the rib (see Fig. 3.6).

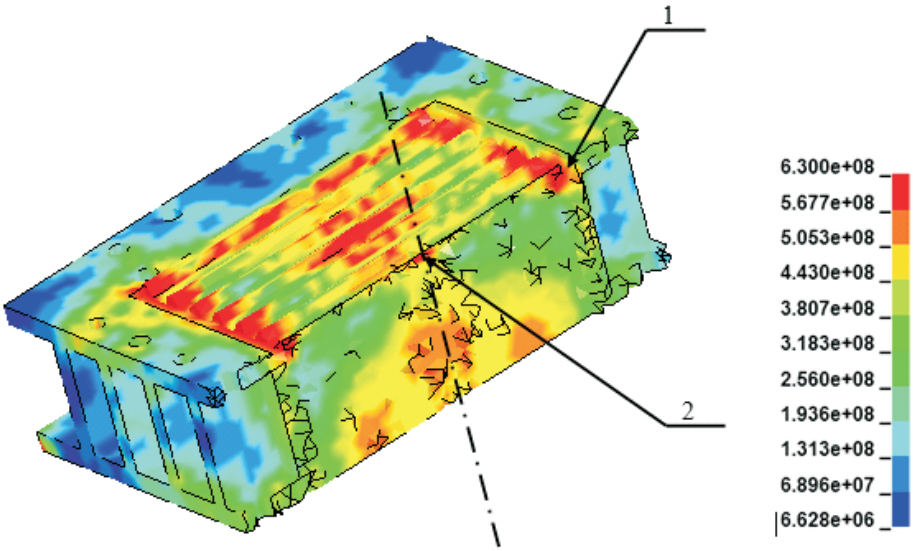

Fig. 3.7. Distribution of stresses in the stopper rib cross-section

3.3. Collision of the basic valve ribs

Collision of the moving grate with the stopper grate is a natural phenomenon occurring during the closing of the valve. Therefore, the dynamic reaction of the stopper rib was analysed using the SWM and the obtained results were verified experimentally.

Due to the operating conditions of the valve, the impact of moving grate ribs against the stopper grate rib at a velocity of 1 m/s was considered. The moving rib was assumed to be a non-deformable mass. Before the impact, the stopper ribs were at rest. The change in the acceleration of the stopper rib over time was examined in the analysis. The calculations included the damping ratio $\xi = 0.006$. Fig. 3.8 presents the change in acceleration over time obtained as a result of numerical calculations.

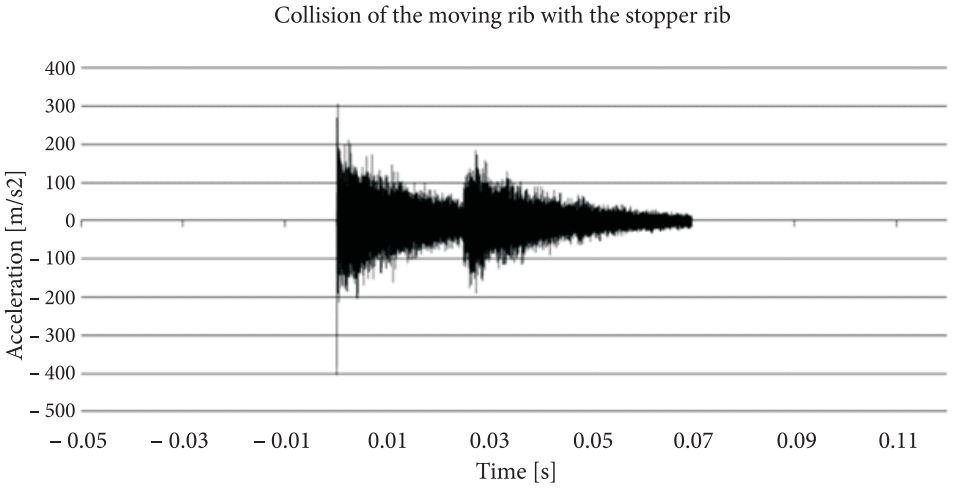

Fig. 3.8. Graph of acceleration of the moving rib over time (obtained as a result of numerical calculations by stress wave method)

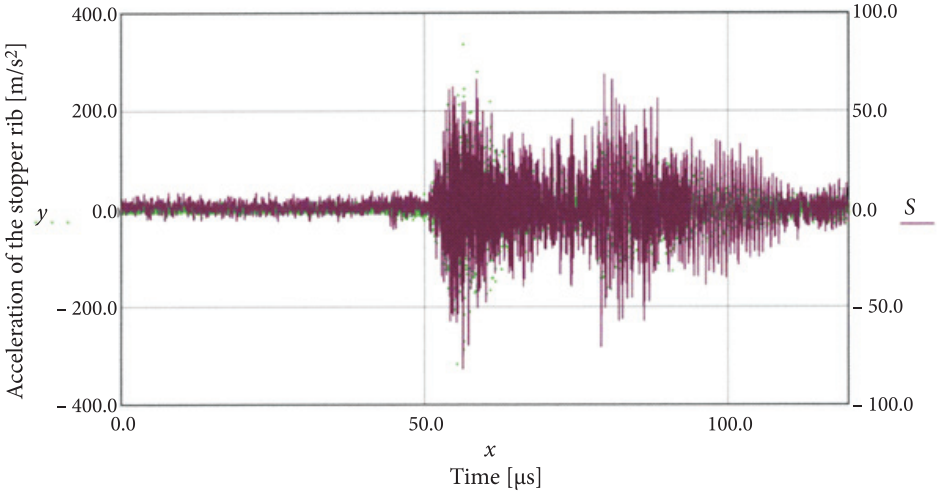

Fig. 3.9. Graph of acceleration of the moving rib over time (obtained as a result of the conducted experiment)

A set of equipment was used to measure the vibrations of the grate, including: PCB accelerometer model JM353B15, 482A16 amplifier and power unit, Yokogawa DLM 2054 four-channel digital oscilloscope, data recording and analysis software (Xviwer, SigmaPlot 10.0, Mathcad14). The oscilloscope recorded 6,250 samples per second. Other details of the test are provided in the report [13]. The results of the experiment are shown in Fig. 3.9. We conclude that the results obtained numerically

are generally consistent with the results of the experiment. These results indicate a two-phase nature of the valve closure. It was found that, in all of the conducted measurements, there are two consecutive excitations of acceleration of the stopper rib. Thus, it is possible to distinguish the time of the first contact of the grate with the stopper rib and the time of full closing of the valve.

4. Summary and conclusions

The structural elements of an explosion-proof valve are one of many examples where the load under working conditions is dynamic. Therefore, the ability to predict the reaction of structural elements and systems to this type of load is particularly important for their design. This reaction depends on many factors. Due to the complex nature of the issue, very often such a reaction can be predicted only by numerical analysis.

The paper presents the concept of determining the dynamic reaction of structural elements using the SWM. The SWM makes it possible to take into account the wave nature of stress development in structural elements and systems subjected to dynamic impacts. The method fully reflects the physics of material and surface waves. The general reaction of a structural element or system and the local effects are determined as a result of a simulation of wave processes within a given space of a structural material with its constraints. It was shown in the paper that the results of calculations using the SWM are generally consistent with the results obtained by means of commercial FEM programs, as well as with the results of experimental tests. Due to the non-stationary nature of the wave process, results may display inconsistencies with respect to the solutions obtained based on algorithms that disregard this fact, which was found in the central cross-section of the analysed valve rib.

The concept of determining dynamic reaction using the SWM presented in the paper can be used for advanced analyses carried out for practical and theoretical purposes in the field of structural dynamics. A significant advantage of the discussed method that should be emphasized is its open nature, which offers a wide range of opportunities for further improvement.

Work financed as part of the statutory activity of the Military University of Technology and the PBR 219/2007 grant.

Received October 18, 2018. Revised December 7, 2018.

Paper translated into English and verified by company SKRIVANEK sp. z o.o., 22 Solec Street, 00-410 Warsaw, Poland.

REFERENCES

[1] Bąk G., Szcześniak Z., *Metoda modelowania dyskretnego jednowymiarowych procesów falowych w sprężystych warstwowych prętach niepryzmatycznych*. Engng. Trans. 35, 2, PAS, IFTR, Warsaw,1987, s. 309-325.

[2] Bąk G., *Bezpośrednia metoda różnicowa w dynamice konstrukcji sprężystych, Mechanika i komputer*, T. 5, Wydawnictwo PAN IPPT, Warszawa 1983, s. 159-175.

[3] Bąk G., Stolarski A., *Analiza nieliniowa prętowych ustrojów żelbetowych obciążonych impulsowo*, Studia z zakresu inżynierii, PAN KILiW, Warszawa, 1990.

[4] Bąk G., *Metoda kinematyczna w zagadnieniach dynamiki konstrukcji sprężysto-plastycznych*, Dodatek do Biuletynu WAT, 7, 347, 1981.

[5] Campbel J. D., *The dynamic yielding of mild steel*, Acta Metallurgica, 1, 1953, s. 706-710.

[6] Kaliski S., Rymarz C., Sobczyk K., Włodarczyk E., *Vibrations and waves*, Part B: Waves, ed. S. Kaliski with L. Solarz, vol. 308 Studies in applied mechanics. Elsevier, 1992.

[7] Krzewiński R., *Dynamika Wybuchu, Część 1, Metody określania obciążeń*, WAT, Warszawa 1982.

[8] Krauthammer T., *Modern protective structures*, CRC Press, Taylor & Francis Group, University of Florida, 2008.

[9] Nowacki W.K., *Stress waves in nonelastic solids*, Pergamon Press, Oxford, 1978.

[10] Stolarski A., *Dynamic Strength Criterion for Concrete*, Journal of Engineering Mechanics, ASCE, December 2004, p. 1428-1435.

[11] Szcześniak Z., Mierczyk Z., Zygmunt M., Wasilczuk J., Wrzesień S., Bąk G., Frant M. i in., *Schronowy zawór przeciwwybuchowy typu automatycznego nowej generacji*, [w:] *Ochrona przed skutkami nadzwyczajnych zagrożeń*, [red:] Z. Mierczyk, R. Ostrowski, t. 2, WAT, Warszawa, 2011, s. 699-766.

[12] Szcześniak Z., Pieńko B., *Metoda analizy dynamicznej podstawowych elementów konstrukcyjnych schronowych zaworów przeciwwybuchowych*, [w:] *Ochrona przed skutkami nadzwyczajnych zagrożeń*, [red:] Z. Mierczyk, R. Ostrowski, t. 1, WAT, Warszawa, 2010, s. 409-421.

[13] Szcześniak Z., Wrzesień S, Piotrowski W., Pieńko B., *Sprawozdanie końcowe z realizacji pracy badawczej PBR 219/2007 pt. „Automatyczny zawór przeciwwybuchowy nowej generacji"*, Warszawa 17.07.2010.

[14] Szcześniak Z., *Spatial discrete structure model for simulation of wave propagation in solids*, Volume of Abstracts 33rd Solid Mechanics Conference, Polish Academy of Sciences, Warsaw – Zakopane, 2000, s. 381.

[15] Szcześniak Z., *Modelowanie zachowania dynamicznego konstrukcji podziemnych w warunkach działania powietrznej fali uderzeniowej*, Wydawnictwo WAT, Warszawa 1999.

[16] Alvarez R., Molina J., Nowacki W. K., Alarcone E., *Los metodos de las caracteristicas y elementos finitos en propagation des ondas*, Ingenieria Mecanica, 2, Madrid, 1985.

[17] Courant R., Friedrichs K., Lewy H., *Uber die partiellen differenzengleichungen der mathematischen Physik*, Math. Ann. 100, 32, 1928, pp.32-74.

[18] http://fgg-web.fgg.uni-lj.si/~/pmoze/esdep/master/wg02/l0310.htm, Lecture 2.3.1: Introduction to the Engineering Properties of Steels (data dostępu 07.12.2018).

B. PIEŃKO, Z. SZCZEŚNIAK

Metoda fal naprężeń w analizie odporności dynamicznej zaworu przeciwwybuchowego

Streszczenie. W artykule przedstawiono koncepcję metody wyznaczania reakcji dynamicznej elementów konstrukcyjnych zaworu przeciwwybuchowego. Zaproponowano metodę fal naprężeń (MFN). Metoda fal naprężeń stanowi oryginalną propozycję rozwiązania zagadnienia reakcji dynamicznej elementów i ustrojów konstrukcyjnych. Jest szczególnie wskazana w przypadkach występowania intensywnych oddziaływań typu udarowego lub wybuchowego. Metoda została opracowana przez autora prac [14, 15]. Umożliwia odzwierciedlenie falowej natury ewolucji naprężeń. W artykule przedstawiono genezę, sformułowano założenia i podstawowe zależności metody. Charakterystykę właściwości omawianej metody zilustrowano rozwiązaniami zagadnień związanych ściśle z wymaganiami w zakresie badań odporności schronowych zaworów przeciwwybuchowych. W ramach charakterystyki wykonano również porównanie wyników obliczeń z wynikami otrzymanymi za pomocą MES a także z wynikami badań doświadczalnych. Wykazano możliwość występowania istotnych różnic pomiędzy porównywanymi rozwiązaniami. Warto podkreślić, że naturalne dla dynamicznej reakcji elementu a więc dla procesów falowych jest tłumienie geometryczne, odbicia i interferencje fal. Zjawiska te mogą istotnie wpłynąć na dystrybucję w przestrzeni i w czasie parametrów poszukiwanej reakcji dynamicznej. Zaproponowana metoda analizy wyróżnia się wysoką dokładnością obliczeń.

Słowa kluczowe: fale naprężeń, drgania elementu konstrukcyjnego, modele dyskretne, rozwiązanie różnicowe, zawór przeciwwybuchowy

DOI: 10.5604/01.3001.0012.8497